A Study on Adopting Λ-Shape Groove for Laser-Arc Hybrid Welding to Construct Thick Plate Butt Welded Joints

Uchino, Issei
Namura Shipbuilding Co., Ltd

Uemura, Takamori
Department of Civil and Structural Engineering, Graduate School of Engineering, Kyushu University

Gotoh, Koji
Department of Marine Systems Engineering, Faculty of Engineering, Kyushu University

https://hdl.handle.net/2324/6786332

出版情報：Welding International. 34 (7/9), pp.357-371, 2021-07-05. Taylor & Francis Group
バージョン：

A Study on Adopting Λ-Shape Groove for Laser-Arc Hybrid Welding

to Construct Thick Plate Butt Welded Joints

UCHINO Issei*, UEMURA Takamori** and GOTOH Koji***

*Namura Shipbuilding Co. Ltd.
**Student Member, Graduate School of Engineering, Kyushu University
***Member, Department of Marine Systems Engineering,
Faculty of Engineering, Kyushu University

Most Japanese shipyards that build general merchant ships use arc welding, but they always have the problem that the accuracy of the hull construction is poor as a result of the thermal deformation caused by arc welding. As one method to overcome this problem, it is expected to adopt laser arc hybrid welding that can suppress the total heat input as a result of heat input concentration, but the initial introduction cost is high and this welding method has a poorer gap tolerance than conventional arc welding. In addition, few experiences to apply laser arc hybrid welding for constructing the joints at the plate thickness level used for hull members of general merchant ships. An improved procedure to fabricate a butt joint with a plate with a thickness of 15 to 20 mm, which is widely applied as a hull member of general merchant ships, is proposed in this study. Proposed procedure is that the Λ-shaped groove with a very small angle and one-pass welding by laser arc hybrid welding with CO_2 gas shielded arc welding to satisfy the weld reinforcement on the front side weld bead. The joint quality manufactured by using our proposed procedure was confirmed according to the Guidelines for Laser Arc Hybrid Welding by a classification society Nippon Kaiji Kyokai (ClassNK). It is expected to be introduced as an alternative method of plate joint welding for hull members, especially submerged arc welding with large heat input.

Key Words: Laser-arc hybrid welding, Welding construction method, Shipbuilding, Butt welding, Groove shape, Quality of welded joint

1. Introduction

The major products of Japanese shipyards are tankers that carry crude oil, coal or iron ore and general commercial ships such as bulk carriers, and arc welding, including CO_2 gas shielded arc welding, shielded metal arc welding, submerged arc welding and electrogas arc welding, is used in the hull construction process. With the increasing size of ships and the development of welding methods, the production capacity of the shipyards has increased dramatically. However, deformations caused by welding and the work to correct them reduce the accuracy of hull blocks in the subsequent process. Therefore, shipbuilding engineers recognize that reducing of welding deformation is an on-going issue.

In the hull construction process, welding methods that can minimize weld deformation are required. The thickness of the structural members that support the strength of a general merchant ship is more than 10 mm, and the joint length of the butt weld is more than 20 m. Therefore, it is necessary to keep the root gap allowance at about 2 mm during construction. Since, however, general merchant ships are built as one-off products and are subject to international construction cost competition, high power laser welding and electron beam welding, which are known to produce little welding deformation, are not realistic options considering the cost of installing the equipment. On the other hand, laser arc hybrid welding (hereinafter simply 'LAHW'), a combination of the advantages of laser welding which can effectively reduce weld deformation with conventional arc welding, which has excellent gap tolerance, is a breakthrough measure that is expected to provide a solution. A comparison between hybrid welding and conventional arc welding shows that, since lasers are capable of applying high energy locally, it is possible to produce joints with relatively little welding deformation. This has been the subject of considerable study overseas[1-4] and it is widely applied in shipyards that construct ships such as passenger liners[5]. In recent years, the introduction of contents of some of the research into this method in Japanese shipyards have been reported[6,7] but its use in actual vessels is limited to joints of relatively thinner steel plate, such as in passenger ships, PCC (Pure Care Carrier) and patrol boats, than those used in commercial shipping[8,9].

Since laser welding is capable of adapting to the groove tolerance allowable during the current hull construction process, even during groove machining there is no need for comparatively costly processes such as mechanical cutting and laser cutting, but in order to use hybrid welding to join the thick plates that form the hull of a general commercial ship, it is necessary to make it applicable to the plate thicknesses and joint lengths at the hull strength member level. Also, since, if the safety of laser processing workers, there is a requirement to separate off the location where hybrid welding is carried out by light shielding etc., automatic operation by, for example, a robot must be used. If we consider the hull structure with the above considerations, it can be expected that this method will come into use for processes such as plate joint welding of the parallel parts of the hull, where joining stiffeners to the plates of the parallel part, even taking the initial setup costs into account, should be expected.

In this study, which takes the above research background into consideration, we report on the results of an examination of the conditions, particularly the groove shape, for butt joining to connect the plates of hull parallel parts. High speed multiple electrode one-sided submerged arc welding is often used in the production of the butt joints considered here, but since this is continuous high heat input welding, it often results large angular distortion, and it is in the solution of this problem for hull construction processes that the advantages of LAHW can be expected to be most evident. As for the range of plate thickness that was studied, an examination of the plate joint welds in the ships of the scale produced in the shipyard to which one of the present authors belongs showed that 20mm or less occupied 65% of the weight ratio and it was decided to study this thickness. Joint quality was assessed

‘Guidelines on Laser-Arc Hybrid Welding (Third Edition)’[10] stipulated by the Nippon Kaiji Kyokai (ClassNK) (hereinafter: ‘the Guidelines’).

2. Test materials and welding equipment

The test materials were KA32 (15mm thick) and KA36 (20mm thick) rolled steel plates for hulls, which is approved by ClassNK. The chemical composition and mechanical properties of these are shown in Table 1. The principal object of the present research was to gather findings that would facilitate the application of hybrid welding to conventional shipbuilding processes, so the test materials were coated to a target thickness of 0.015mm with the inorganic zinc coating known as ‘shop primer’ for rust prevention during construction and the grooving processes were performed using plasma cutting following general shipyard practice.

The configuration of the hybrid welding test apparatus used in these tests is described below. The laser oscillator was fibre laser with a maximum power of 20kW and the arc power source was a digital inverter-controlled type. The laser head and arc torch are held by an articulated manipulator. The welding position is taught prior to installation as multiple points on the weld line including the beginning and end. For this purpose, a CCTV camera attached to the end of the manipulator is used. The equipment is shown in Fig.1.

3. Examination of the welding conditions

3.1 Welding processes with an I-shaped groove

The authors have previously reported[11-13] that it was possible to manufacture butted joints with an I-shaped groove by LAHW up to a plate thickness of 17mm. In these previous reports in which the groove was made by gas cutting or plasma cutting, a sound joint could be made with the test materials when the groove was cut by laser, but as part of the back bead had a poor appearance due to the effects of root gap variation along the weld line, caused by the problems with cutting accuracy, and the state of the groove surface, it becomes clear that it would be difficult to assure the level of joint quality required in shipbuilding. In addition, in preparatory tests carried out before this study, joints with a weld length of 1,000mm were made using KA32 (15mm plate thickness), a good bead appearance on both the front and back surfaces was achieved only very rarely. In the experiment, as in the previous studies, the reason was thought to be due to variations of the root gap of the groove made by plasma cutting. The welding conditions of the preliminary tests resulting in comparatively good front and back bead appearance are shown in Table 2 and the appearance of the front and back beads made under these conditions are shown in Fig. 2. Fig. 3 shows the distribution of the groove widths before welding of the joint at measured intervals of 0.2mm in the longitudinal direction of the weld line using a triangulation-type two-dimensional laser displacement sensor.

DCEN (DC Electrode Negative) type CO_2 gas arc welding[14-16], using REM-added wire, was used as an arc heat source for I-shaped groove butt welding. The reason for this was that a suitable back bead appearance was achieved by setting a higher voltage in the welding condition [11]. On the other hand, the previous study[16] on the superiority of DCEN carbon dioxide arc welding with REM-added wire in hybrid welding reported that a large amount of spatter is generated and a poor front bead appearance is formed when normal welding materials are treated with high voltage. Therefore, with a simple I-shaped groove, the welding conditions become more severe as the plate thickness increases, and it is therefore considered difficult to realize long joints of thick plates, which is the main objective of this research.

3.2 Investigation of Λ-shaped groove welding conditions

It was concluded from the results of multiple preliminary tests that it was difficult to form a stable back bead with an I-shaped groove, but it was notable in some of the preliminary tests that in the test materials with which a back bead of relatively good appearance was obtained, the root gap was open at back side after tack weld. In hull construction processes, however, the joint length is more than 20m long and it is therefore practically impossible to make appropriate settings for the root gap preparation and it is preferable to have construction guidelines that specify that the cut steel sheets are simply to be adjacent to each other.

Considering the above-mentioned problems at the shipyard, it was decided to set a very small cutting angle using an NC plasma cutting machine to cut out a Λ-shaped groove once only from the weld front surface (or an inverted V-shaped groove with the groove opening onto the weld rear surface). The plate joint of the hull parallel part described in the present study being in the most upstream location of the construction process, complex groove operations affect the progress of the work but since with this cutting method the cut top surface aligns with the top surface of the weld, there is no need for the steel plate to be reversed. Fig. 4 shows a photograph of the cross section of the cut groove butted together before welding. Since the nozzle is closer to the material surface than when cutting the V-shaped groove used in conventional arc welding, part of the upper edge of the bevel is also melted. This results in an X-shaped groove shape when the groove shape cross sections are butted together. The setting information of the NC plasma cutting machine when this beveling process was carried out is as follows: the cutting angle is 3° for a plate thickness of

15 mm, and 2° for a plate thickness of 20 mm. Tests using test materials of KA32 (15mm thick) and KA36 (20mm thick) and a weld length 300mm were performed to find the welding conditions for a Λ-shaped groove. LAHW involves innumerable combinations of conditions depending on the parameters of the laser and arc, so the welding conditions shown in Table 3 were fixed and only the three conditions of arc current and voltage, travel speed and laser power were allowed to be varied as part of the research.

The validity of the welding conditions was judged by qualitative assessment of the appearance in four grades of back bead appearance and three grades of spatter production and the criteria for these judgements are shown in Fig. 5 and the experimental results in Figs. 6 to 8.

As a result of welded joints with different root gaps, based on I-shaped groove welding conditions already found in previous studies, a good back bead appearance was obtained at the laser power of 10kW for a plate thickness of 15mm and at 14kW for a plate thickness of 20mm. Whereas the appearance was good even when the root gap on the back side was 1mm, test materials with a narrower gap showed either a convex bead or humping at the same laser power. This is thought to be due to a space being created at the back side of the groove by the root gap, with the reduction of the excess weld metal that would have become convex.

Next the current and travel speed were optimised with the laser power fixed. The amount of deposited metal, represented by the vertical axis in Fig. 7, was calculated from the wire feed amount, wire diameter and welding speed determined by the arc current with the assumption of 100% deposition efficiency. For example, with the thinner plate (15mm) at a fixed current of 300A and welding speed of 1200mm/min, as shown in Fig. 6, the amount of deposited metal was 102mm^3/cm. With both plate thicknesses, it was clear that a good back bead appearance was achieved when the amount of deposited metal was kept to around 100mm^3/cm, with a root gap in the range 1~1.3mm. Also, the results for a plate thickness of 15mm and a root gap of 1mm show that there was little deposited metal; in other words, small current and high travel speed achieved good results. Further, with a larger gap of 1.3mm, the amount of deposited metal, which is varied by changes in arc current and travel speed, was 80~120mm^3/cm over the complete range, with a good back bead appearance. This is also thought to be the effect of an increase of space in the groove back side and reduction of excess deposited metal and indicates the superiority of the Λ-shaped groove.

Finally, the choice of arc voltage is discussed.

For the same arc current, a higher voltage will give a better bead appearance, but will also increase the amount of spatter. Decreasing the voltage at the same arc current value increases the arc force and results in a "buried arc" condition. As a result, spatter is reduced, but the penetration becomes deeper and a convex back bead is formed. Fig.8 shows a case in which the arc current is set to 350A, the welding speed is 1300mm/min and the amount of deposited metal is held down to 122mm^3/cm. It is clear from this that a good back bead can be formed if the laser power and the amount of deposited metal are set according to each root gap and the voltage is set according to the current. It was aimed to improve the bead appearance by using DCEN type CO_2 gas arc welding in which REM-added wire is used with I-shaped groove butt joints, but it was significant that, when a Λ-shaped groove was used, a good appearance could be obtained by the CO_2 gas arc welding conventionally used in shipbuilding. However, the quantity of deposited metal was less with a groove with space on the back side and maintaining the same amount of deposited metal with greater plate thickness had the adverse effect of insufficient metal for the front bead, as shown in Fig. 9.

In the panel plate-joining process of hull parallel parts, the quality of the back bead is regarded as more important than that of the front bead. This is because when the front bead is repaired, repair welding is possible in the flat (PA in ISO 6947) direction, but the back bead requires repair welding in an overhead (PE in ISO 6947) direction which involves an increase in the number of processes. Therefore, in the present research, emphasis was placed on the formation of a good back bead by LAHW and if there was a deficiency of deposited metal in the front bead, this was dealt with by repair welding by CO~~2~~ gas arc welding. 1.2mm flux cored wire (JIS Z 3313: T 49J 0 T1-IC A-U), which is generally used in repair welding in shipyards, was used and the process was carried out using a rail-travelling auto-moving carriage again, as often used for cutting and welding at shipyards as shown in Fig. 10. An example of the weld bead appearance after repair is shown in Fig. 11. Fig. 12 shows a concept for the future introduction of LAHW into hull construction processes, the arc torch for repair welding fitted to the rear of the LAHW and where the travel speed for the repair welding is the same as for the LAHW.

4. Fabrication of a 1,000mm specimen

4.1 Welding conditions and bead appearance

A butt joint specimen with a weld length of 1,000mm, necessary for approval as a welding process by the Classification Society, was fabricated with laser power based on the power derived from experiments with a welding length of 300mm and with a relationship between arc current and welding speed for a fixed amount of deposited metal. The test piece was tack welded (with extremely short tack welds less than 10mm in weld length) by CO_2 gas arc welding at the centre and at positions approximately 50mm from the starting and terminal ends of the LAHW, and tab pieces were attached to the edges with weld lengths of 50mm so as not to impinge on the weld line. The tack welding is shown in Fig. 13. The root gap widths measured by laser scanner after tack welding are shown in Fig. 14. The measuring equipment and measurement intervals were the same as for the measurements shown in Fig. 3. The welding conditions for the specimens under which a good bead appearance was obtained are shown in Table 4. The conditions shown in Table 3 are used for the welding conditions not shown in this table. Since, in this experiment, grooves were made in the test pieces by plasma cutting, there were differences between individual root gaps and the conditions were adjusted slightly to improve the appearance of the back bead. Also, root gap variance in the weld line direction is expected to be more markedly apparent in shipyards, where lengthy welding is carried out, and a system capable of real-time control of conditions according to the root gap is a project for the future. The great progress in image processing technologies made in recent years has made tracking control and in-process penetration measurement possible[17,18]. It is expected that processes capable of adapting to variations in the groove will be developed by combining these technologies. Furthermore, travel speed under these conditions was 1.3-fold the speed of the multiple electrode one-sided submerged arc welding used for the joining of hull parallel parts, so there are also advantages in terms of efficiency due to improvement in travel speed.

The back bead appearance after welding was good for both a plate thickness of 15mm and a plate thickness of 20mm but, as in the case of the specimen with the weld length of 300mm, the build-up on the front side was inadequate. Accordingly, as described above, repair welding was carried out by CO_2 gas arc welding. The bead appearance after this repair welding is shown in Fig. 15 for the 15mm thick plate and in Fig. 16 for the 20mm thick plate. It is clear from Figs. 15 and 16 that good bead appearances can be achieved.

4.2 Non-destructive inspection results

Ultrasonic testing (UT) and radiographic testing (RT) were performed on the 1,000mm butt joints fabricated. The test conditions are shown in Table 5. The results for the 15mm thick plate are shown in Fig. 17. As shown in Fig. 18, in the joint of 15mm thick plates the back bead appearance shows incomplete penetration in a section of approximately 50mm at the terminal part and the defect was detected at this location by UT and RT. A defect crossing the L line specified by Japan Industrial Standards JIS Z 3060 at the start end was detected by UT but the defect was not confirmed on the film of RT. Specimens and tab pieces of the same thickness were used in the present study and it is thought that defects occurred in the unstable sections where the welding starts and ends, where the welding conditions result in disturbance of the molten pool, which occurred when there is a gap between the tab piece and main specimen and the molten pool passes through the vicinity of the boundary between the test piece and tab piece.

The results of non-destructive testing of the 20mm plate are shown in Fig.19. As in the case of the 15mm thick plate, defects were detected at the start and terminal edges but the defect at the terminal edge was detected by RT alone. A defect was detected by UT at a position 125mm from the start edge but no defect was detected at this position by RT, although an image thought to be a very small amount of lack of fusion was detected at position 300mm from the start edge by RT alone. Differences between the results of RT and UT were also observed in other cases, perhaps because of the narrow bead width, and the widespread introduction of non-destructive testing methods into shipbuilding processes remains somewhat problematic. In order to prevent weld defects occurring at the start and end of welding, it is necessary to perform proper tack welding and tab piece installation, and to set appropriate welding conditions for processing near the start and end of welding.

4.3 Mechanical test results

The test pieces were extracted and mechanical tests were performed after the non-destructive tests of butt joints with a weld length of 1,000mm. The sampling positions of the test pieces are shown in Fig. 20.

4.3.1 Tensile tests

The tensile test samples were worked into U2A, as determined by the Guidelines for the tests. The results are shown in Table 6 and photographs of the test pieces are shown in Fig. 21. All of the results show a tensile strength greater than the minimum specified tensile strength of the base metal required by the Rules for the Survey and Construction of Steel Ships of ClassNK[19] referred to as the criteria for the Guidelines, and they thus comply with these standards.

4.3.2 Side bending tests

The side bending test samples were worked into UB-2, as determined by the Guidelines for the tests. Photographs of the test pieces after the tests are shown in Fig. 22. Good results were seen for the 15mm thick plate but for the 20mm thick plate, in both the samples taken from positions approximately 100mm from the weld start end, cracking occurred at the boundary between the weld and base metal at a position near the weld back side. This is thought caused by incomplete fusion and the position of this coincides with that of the defect detected by ultrasonic testing. No defect was detected at this position by ultrasonic testing but it was thought that there was some very slight lack of fusion. Two samples were taken from the spare material at position 200mm from the weld start edge as 20mm test pieces for additional bending tests and these were retested. The results of these tests are shown in Fig. 23 and no cracking occurred.

4.3.3 Macroscopic cross-sectional observations and Vickers hardness tests

The results of the macroscopic cross-sectional observations and Vickers hardness tests of the joints are shown in Fig. 24 for 15mm thick plates and in Fig. 25 for 20mm thick plate. In the macroscopic cross-sectional observations, it was confirmed that there was good penetration at the boundary with the LAHW and repair welding. In the Vickers hardness tests, when these were performed by HV1 test (so-called micro-Vickers hardness test with indentation load 1kgf), although the maximum hardness was shown in the weld metal in each case, the specification of 380HV or below of the Guidelines was met. According to the guidelines, the test should be performed with HV10 (indentation load of 10 kgf), but the test was performed by HV1. The hardness of the Vickers hardness test can be treated as the same even if the test load is different because of the law of similarity[20]. Therefore, we believe that there is no problem in verifying the results based on the results obtained with HV1.

4.3.4 Impact tests

It has been reported[21,22] that, in impact tests of the butt joints, the phenomenon of fracture path deviation from the notch tip towards the base metal occurs due to the narrow width of the weld metal part, while the Guidelines specify an impact test piece with a side groove, i.e. the side surface is grooved. In these tests too, Charpy impact tests were performed using test samples with side grooves. The results are shown in Table 7 and photographs of test pieces after fracture are shown in Fig. 26. The rules for the type of test metals used require impact tests to be performed at 20°C but even when they were performed at the stricter test temperature of 0°, the results met the specified value of 23J.

5. Conclusion

The findings of this study, in which butt joints were fabricated using 15mm and 20mm thick test materials by LAHW, were as follows.

i. With butt welding with an I-shaped groove prepared by plasma cutting, it was extremely difficult to set conditions due to variations in the root gap even when the plate is 15mm thick and it is necessary to use DCEN CO_2 gas arc welding with REM-added wire. On the other hand, with a Λ-shaped groove that spreads onto the back side, it is possible to control the amount of excess deposited metal, which is a cause of convex bead and humping, and achieve a good appearance relatively easily.

ii. When there is a 1mm root gap at the groove back surface, it is possible to obtain a good back bead by setting the arc current and welding speed to obtain a fixed amount of deposited metal.

iii. The performance of 1,000mm welded joints, in which the bead was reinforced by CO_2 gas arc welding after LAHW, complied with the joint performance requirements of the Guidelines, but a lack of fusion was confirmed by non-destructive testing. It will therefore be necessary to investigate welding conditions with higher margins in order to make this a method that can be used in actual ship construction processes.

References

1) F. Roland, et al.: Advanced Joining Techniques in European Shipbuilding, Journal of Ship Production and Design, Vol. 20, No. 3 (August 2004), 200–210.
2) S. E. Nielsen: High power laser hybrid welding – challenges and perspectives, Conference proceedings, 15th Nordic Laser Materials Processing Conference, 15 (August 2015), 25-27.
3) B. Ribic, et al.: Problems and issues in laser-arc hybrid welding, International Materials Reviews, Vol. 54, No.4 (July 2009), 223-244.
4) G.Turichin, et al.: Hybrid Laser-Arc Welding of the High-Strength Shipbuilding Steels: Equipment and Technology, Physics Procedia , 89(2017),156-163.
5) R. Moeller, S. Koczera: "Shipyard uses laser-GMAW hybrid welding to achieve one-sided welding - New system reforms prefabrication in shipbuilding" the fabricator, November 20, 2003, https://www.thefabricator.com/thefabricator/article/arcwelding/shipyard-uses-laser-gmaw-hybrid-welding-to-achieve-one-sided-welding (accessed on 23 September 2020).
6) T. Yokura , et al.: Approach with Advanced Welding Technology at Shipyard , Journal of The Japan Welding Society, Vol.86 No.7 (2017), 6-10. (in Japanese)
7) T. Watanabe, et al.: Guideline for Development of Innovative Processing – Laser Arc Welding - , Journal of The Japan Welding Society, Vol.87 No.3 (2018), 36-41. (in Japanese)
8) H. Koga, et al.: First Application of Hybrid Laser-arc Welding to Commercial Ships, Mitsubishi Heavy Industries Technical Review, 47-3 (2010), 59-64.
9) R. Kimura, et al.: Application of Laser - Arc Hybrid Welding to Japan Coast Guard Patrol Vessel Large, Mitsui Zosen technical review, 216 (2016), 13-19. (in Japanese)
10) ClassNK. "Guidelines on Laser-Arc Hybrid Welding, (Ver. 3)", Nippon Kaiji Kyokai (2016).
11) K. Gotoh, et al.: Joint Industrial Project on the Introduction of Laser-Arc Hybrid Welding Technology to Hull Construction Process - (Part 2) Influence of Factors on Weldability -, Conference proceedings, the Japan Society of Naval Architects and Ocean Engineers, 28 (2019), 265-269. (in Japanese)

12) K. Gotoh, et al.: Joint Industrial Project on the Introduction of Laser-Arc Hybrid Welding Technology to Hull Construction Process - (Part 4) Construction Trial of Butt Welded Joint with Long Welding Length -, Conference proceedings, the Japan Society of Naval Architects and Ocean Engineers, 28 (2019), 277-282. (in Japanese)

13) K. Gotoh, et al.: Overview of the joint industrial project for practical application of laser-arc hybrid welding in construction of general merchant ships in Japan, In Proceedings of 14th International Symposium on Practical Design of Ships and Other Floating Structures, Session ID. T1-D-3, 2019.

14) T. Kataoka, et al.: Development of Ultra-low Spatter CO2 Gas-shielded Arc Welding Process "J-STAR® Welding", JFE TECHNICAL REPORT, 10 (Dec. 2007), 31-34.

15) H. Sumi, et al.: Application of Narrow Gap Welding Process with "J-STARTM Welding" to Shipbuilding and Construction, JFE TECHNICAL REPORT, 20 (Mar. 2015), 112-117.

16) H. Sumi, et al.: Laser-arc Hybrid Welding using Rem Bearing Wire, Proceedings of the 81st Laser Materials Processing Conference, (May 2014), 29-32.

17) T. Kadoya: In-process Depth Meter(IDM) for Laser Welding, Journal of The Japan Welding Society, Vol.84 No.3 (2015), 6-9. (in Japanese)

18) S. Yamane: Tracking of Welding Using Image Processing, Journal of The Japan Welding Society, Vol.84 No.4 (2015), 35-42. (in Japanese)

19) ClassNK: Rules for the Survey and Construction of Steel Ships Part K-Materials, Nippon Kaiji Kyokai (2019).

20) T. Yamamoto: How to Make a Hardness Test in the Right Way, Journal of the Japan Society for Precision Engineering, 75-10 (2009), 1183-1188. (in Japanese)

21) T. Otani, et al.: Mechanical Characteristics of High Power CO2 Laser Welding Joints of Ultra-fine Grained High Strength Steel, Quarterly Journal of The Japan Welding Society, 21-3 (2003), 425-432. (in Japanese)

22) Y. Hagihara, et al.: Toughness Evaluation of Laser Welds using Side-Grooved Charpy Test, Quarterly Journal of The Japan Welding Society, 25-1 (2007), 165-172. (in Japanese)

Table 1 Chemical compositions and mechanical properties of steel plate used.
(a) Chemical compositions. [%]

Thickness	Grade	C	Si	Mn	P	S	Ceq
15 mm	KA32	0.16	0.45	1.04	0.02	0.003	0.34
20 mm	KA36	0.16	0.23	0.99	0.02	0.006	0.33

(b) Mechanical properties.

Thickness	Grade	Y.P. [MPa]	T.S. [MPa]	EL. [%]	V Notch 0°C Energy[J]
15 mm	KA32	384	516	29	175
20 mm	KA36	389	523	25	206

Table 2 Welding conditions for 15mm. / Groove shape “I”.

Laser power [kW]	10
Defocusing distance from the plate surface [mm]	-5
Laser push angle [degree]	20.0
Welding consumable for Arc welding (JIS specification)	YGW18
Wire diameter [mm]	1.6
Arc current [A]	400
Arc voltage [V]	40.0
Wire extension [mm]	20
Arc drag angle [degree]	40.0
Distance between laser radiation point and arc torch aiming point [mm]	5.0
Travel speed [mm/min]	1200

Table 3 Fixed welding conditions. / Groove shape “Λ”.

Defocusing distance from the plate surface [mm]	-5
Laser push angle [degree]	20.0
Welding consumable for Arc welding (JIS specification)	YGW11
Wire diameter [mm]	1.6
Wire extension [mm]	25
Arc drag angle [degree]	40.0
Distance between laser radiation point and arc torch aiming point [mm]	5.0

Table 4 Welding conditions for specimens welding length is 1,000 mm. / Groove shape “Λ”.

Thickness [mm]	15	20
Laser power [kW]	9	14
Arc current [A]	300	280
Arc voltage [V]	28.0	24.0
Travel speed [mm/min]	1,200	1,100

Table 5 Nondestructive inspection condition.

(a) Ultrasonic inspection.

Applicable code	JIS Z 3060
Disregard level	L level
Test stage	As welded
Technique	Angle beam technique
Probe	5C10 x 10A70
Angle of incidence	70 degree
Couplant	Glycerin

(b) Radiographic inspection.

Applicable code	JIS Z 3104
Test stage	As welded
Technique	Single wall viewing
Tube voltage [kV]	250
Tube amperage [mA]	3
Exposure Time [min.]	1.0
Film size [mm]	85×305

Table 6 Tensile test result.

Thickness [mm]	Steel grade	Requirement [MPa]	Specimen ID	Tensile Strength [MPa]
15	KA32	≧440	1	558
			2	556
20	KA36	≧440	1	590
			2	588

Table 7 Impact test results.

Thickness [mm]	Steel grade	Test temperature [°C]	Requirement [MPa]	Notch location	Absorbed energy [J]			
					Value1	Value2	Value3	Average
15	KA32	0	≧23	Depo.	103	92	73	**89**
				Fusion line	42	40	38	**40**
				FL+2mm	38	35	33	**35**
20	KA36			Depo.	65	76	47	**63**
				Fusion line	57	50	40	**49**
				FL+2mm	33	29	29	**30**

Fig. 1 External appearance of equipment.

(c) Front side.

(d) Back side.

Fig. 2 Bead appearance of 15 mm. / Groove shape “I”.

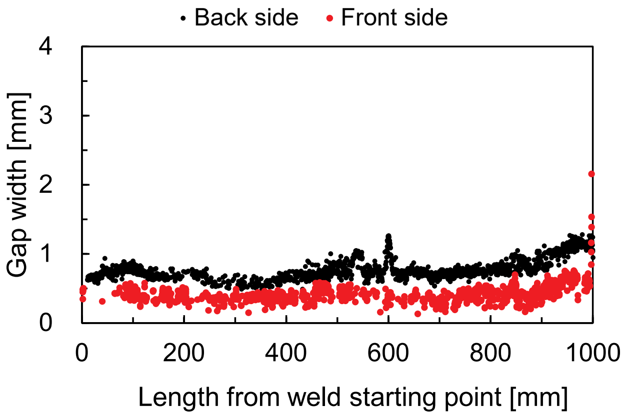

Fig. 3 Gap width profile of 15 mm. / Groove shape “I”.

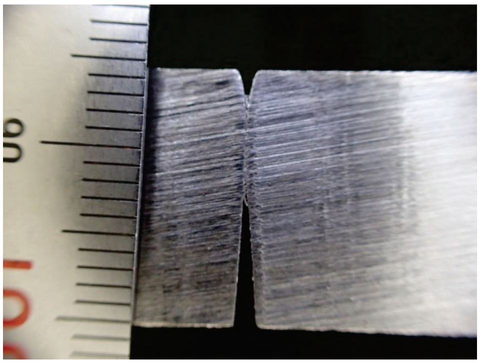

Fig. 4 Cross section of “Λ” groove.

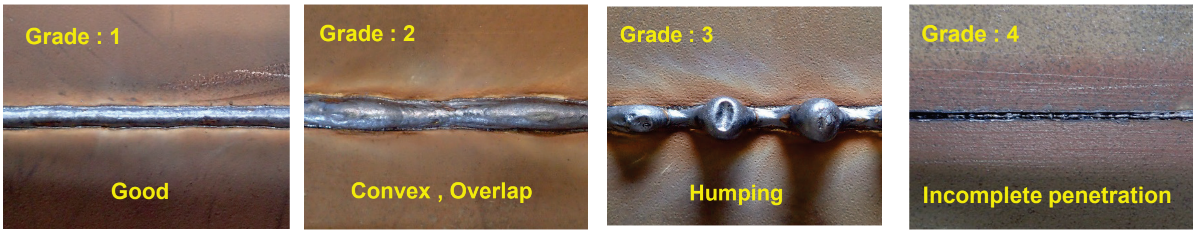

(a) For back bead appearance.

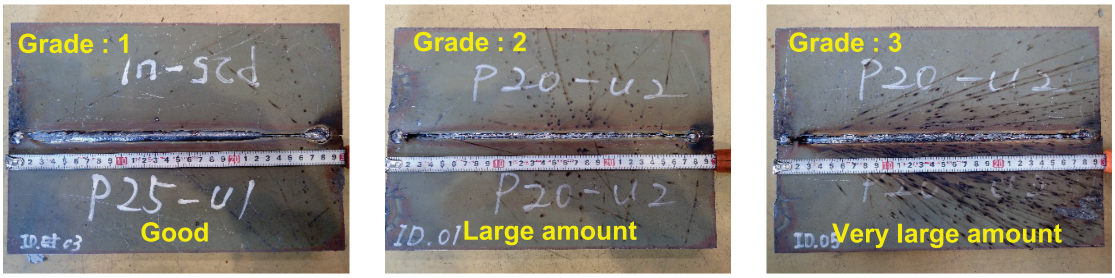

(b) For spatter.

Fig. 5 Evaluation criteria.

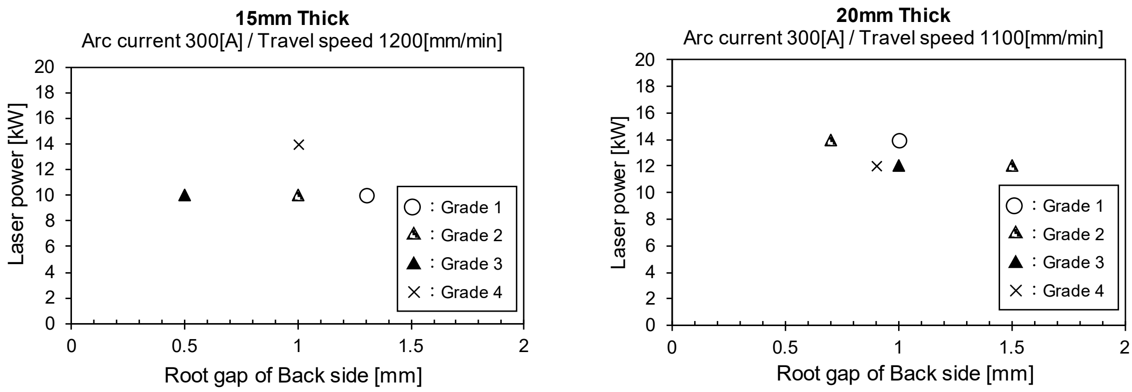

Fig. 6 Effect of root gap on the back side and laser power on back bead appearance.

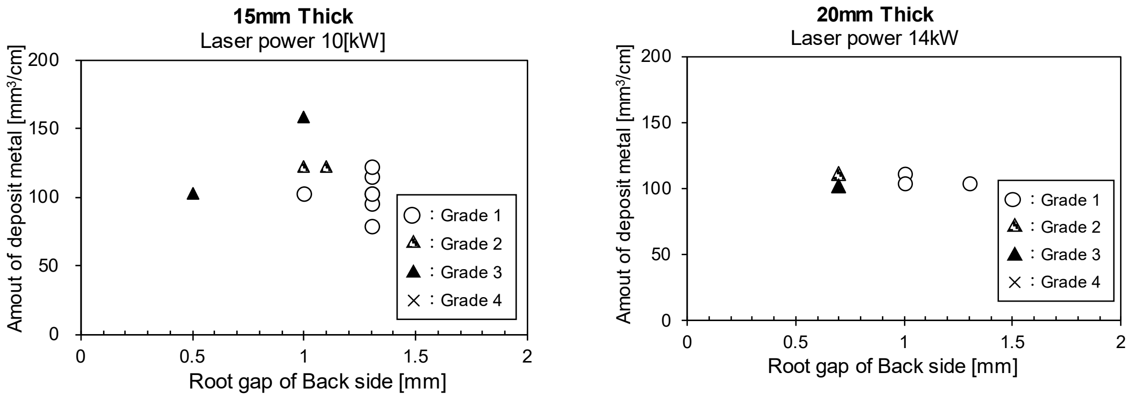

Fig. 7 Effect of root gap on the back side and amount of deposited metal on back bead appearance.

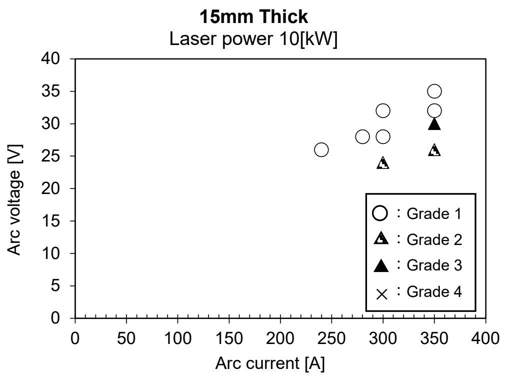

(e) Back bead appearance.

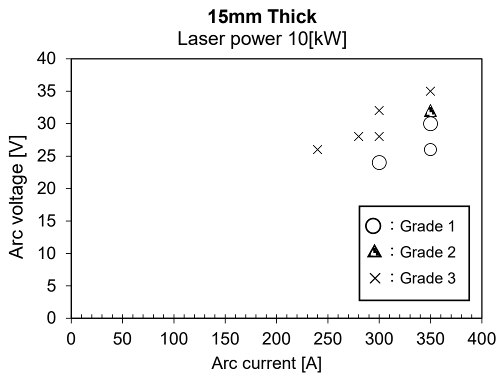

(f) Spatter at front surface.

Fig. 8 Effect of arc current and voltage on back bead appearance.

Fig. 9 Specimens of under fill on the front bead at 20 mm.

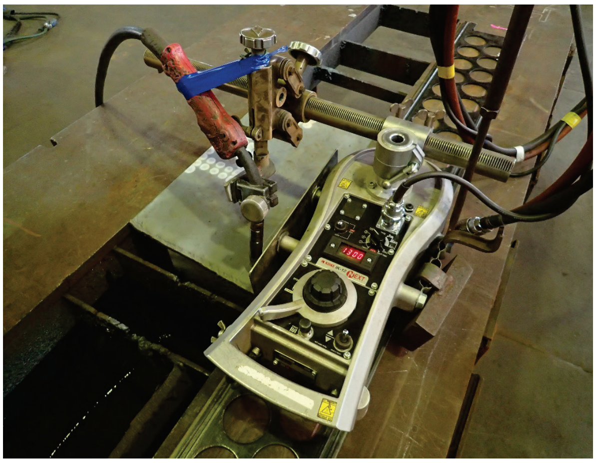

Fig. 10 State of repair welding.

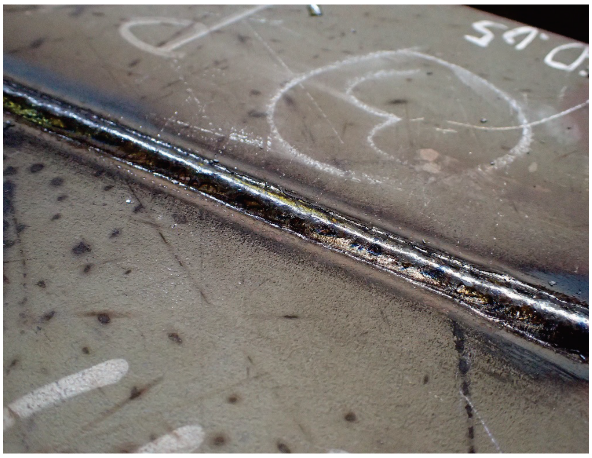

Fig. 11 Repair welding appearance.

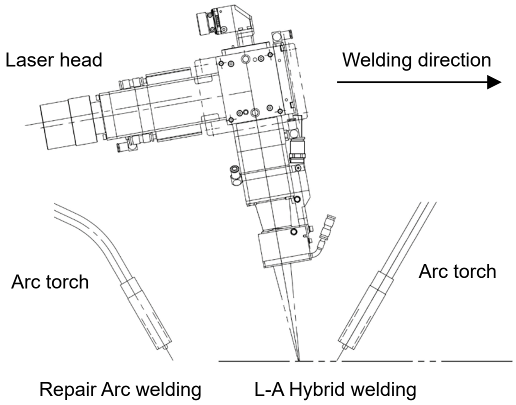

Fig. 12 Schematic illustration of arrangement of laser-arc hybrid welding system that can consistently perform repair of reinforcement by arc welding.

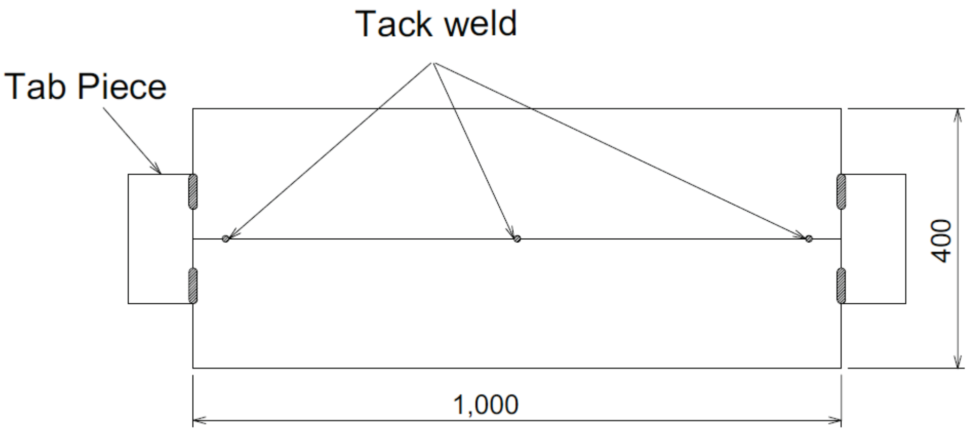

Fig. 13 State of Tack weld.

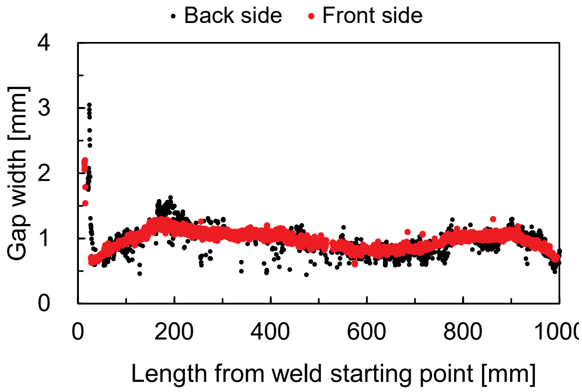

(g) Thickness: 15 mm.

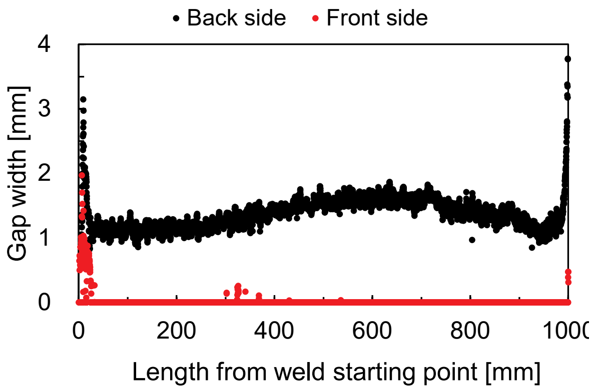

(h) Thickness: 20 mm.

Fig. 14 Gap width profile welding length is 1,000 mm. / Groove shape “Λ”.

(a) Front bead appearance at 200/400/600/800 mm from welding start point

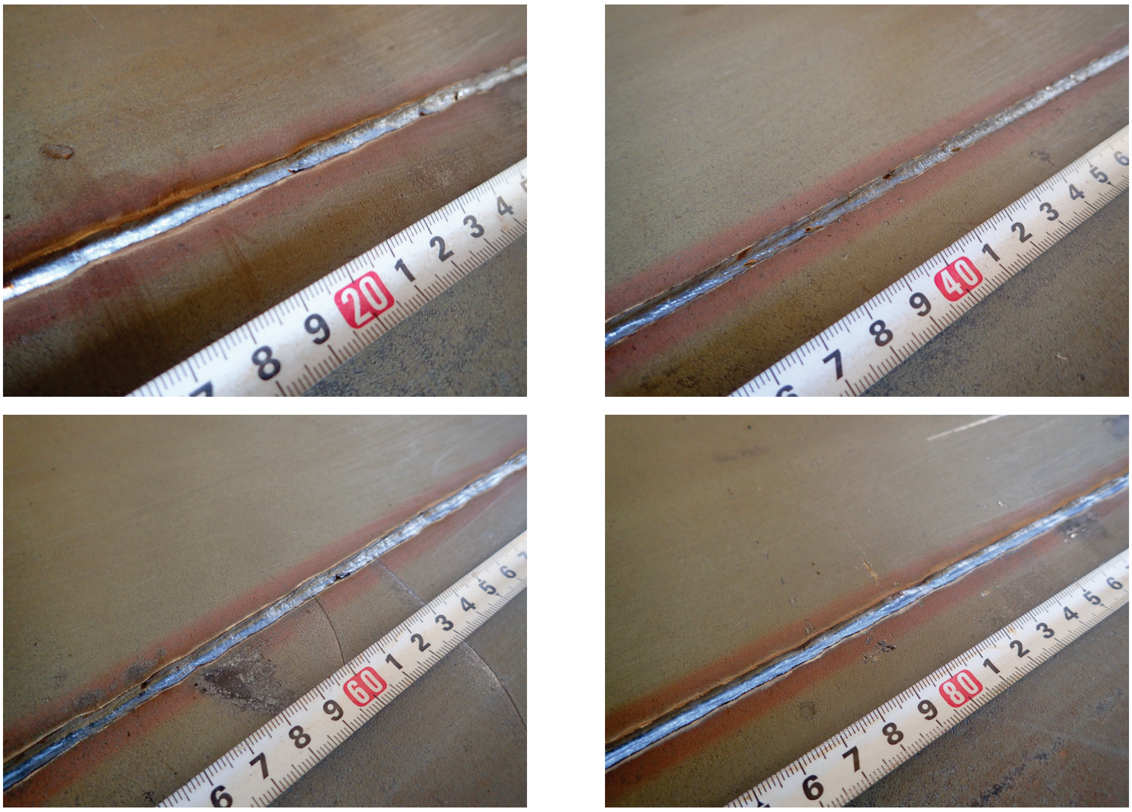

(b) Back bead appearance at 200/400/600/800 mm from welding start point

Fig. 15 Bead appearance at 15 mm-thickness specimens.

(a) Front bead appearance at 200/400/600/800mm from welding start point

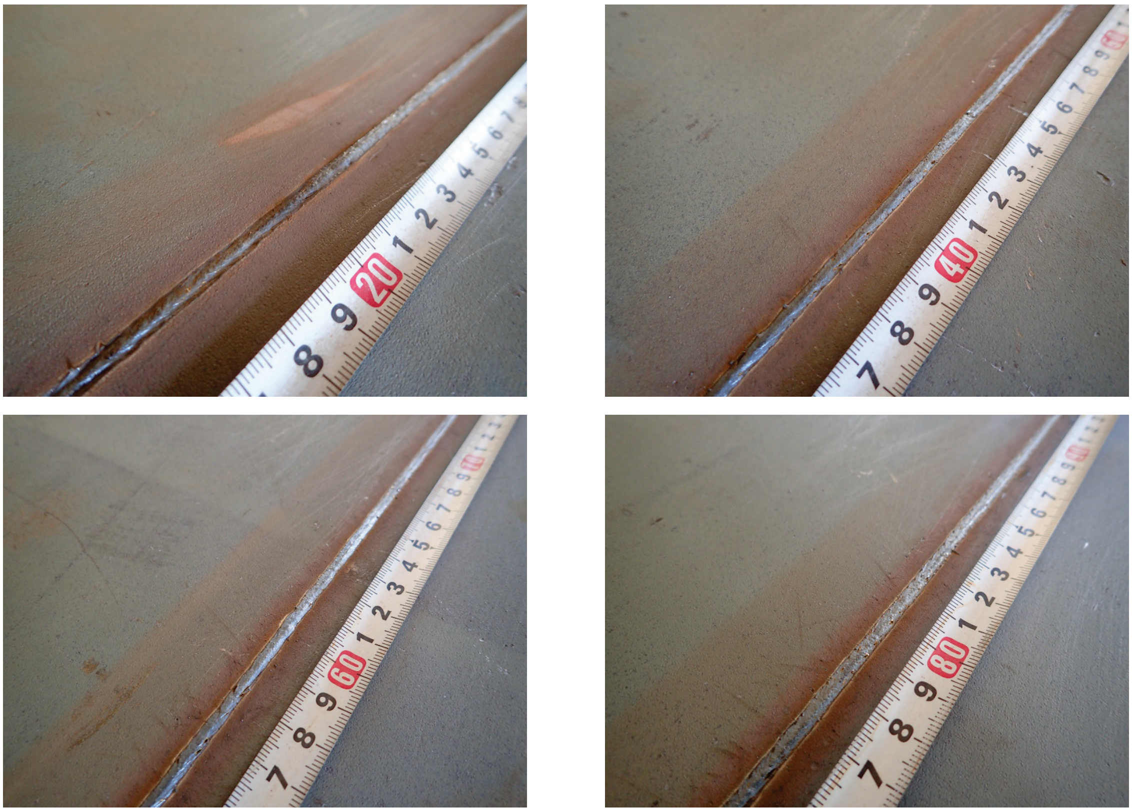

(b) Back bead appearance at 200/400/600/800 mm from welding start point

Fig. 16 Bead appearance at 20 mm-thickness specimens.

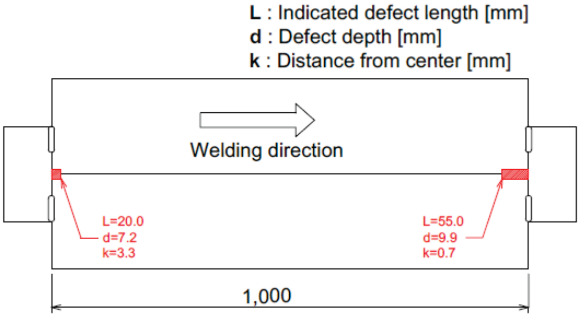

(a) Ultrasonic testing record.

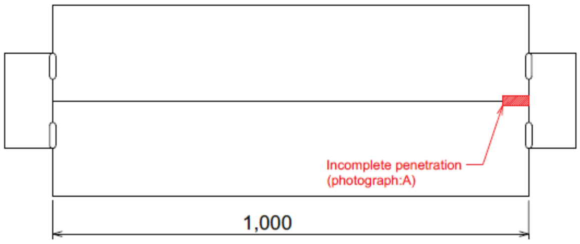

(b) Radiographic testing record.

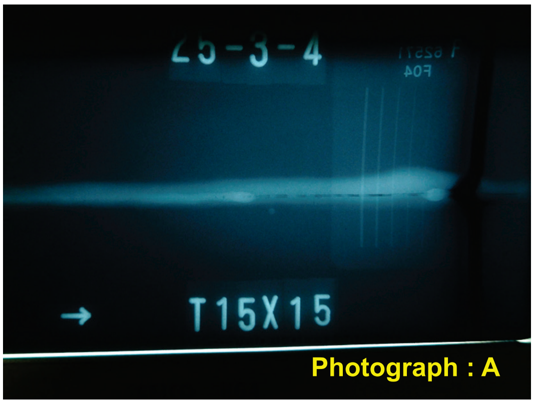

(c) Radiograph.

Fig. 17 Nondestructive inspection result for 15 mm-thickness specimen.

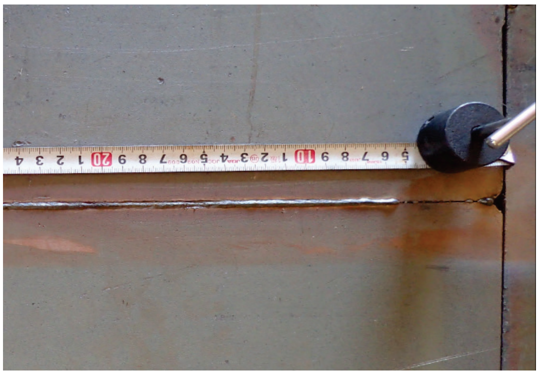

Fig. 18 Lack of penetration of 15 mm-thickness specimen.

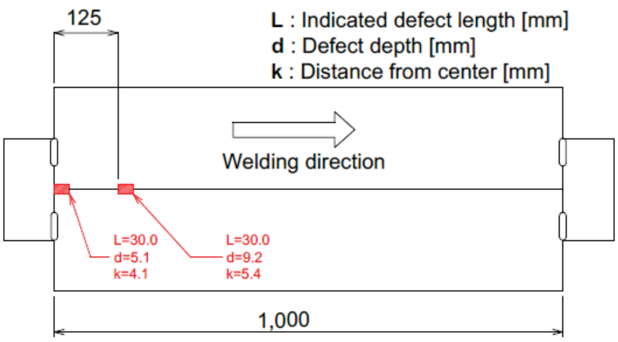

(a) Ultrasonic testing record.

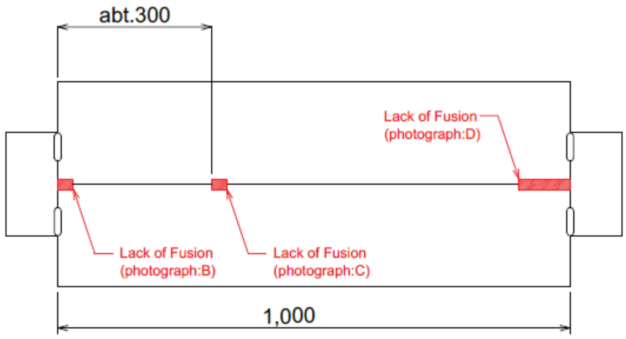

(b) Radiographic testing record.

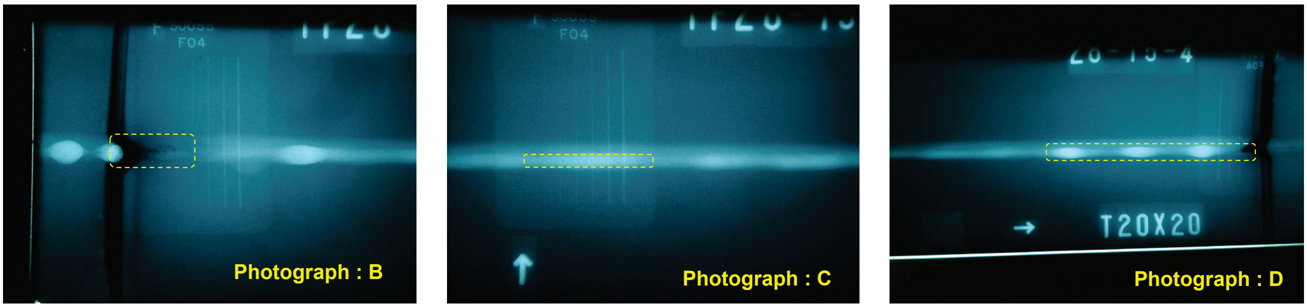

(c) Radiographs.

Fig. 19 Nondestructive inspection result for 20 mm-thickness specimen.

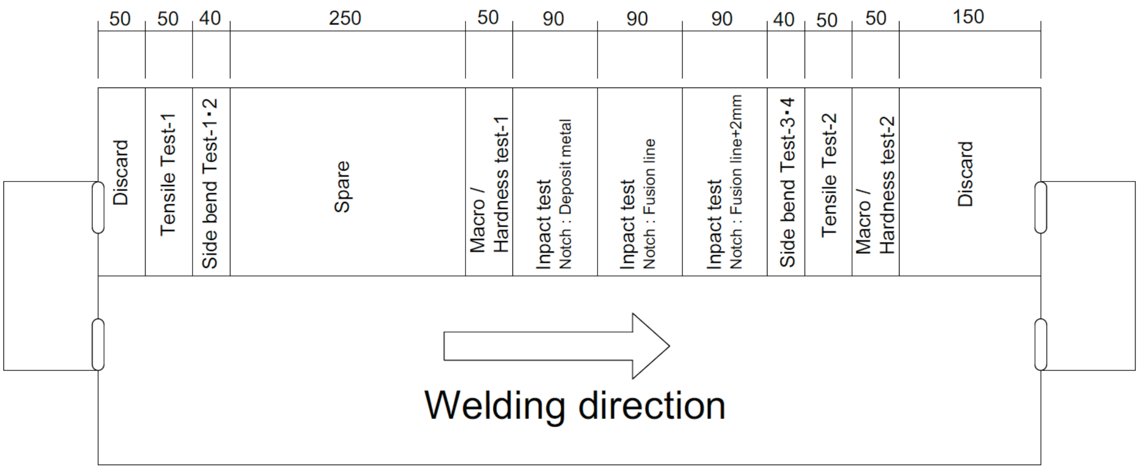

Fig. 20 Mechanical test specimens sampling position.

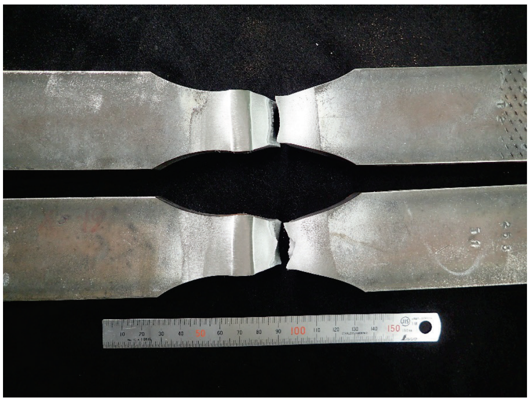

(a) Thickness: 15 mm.

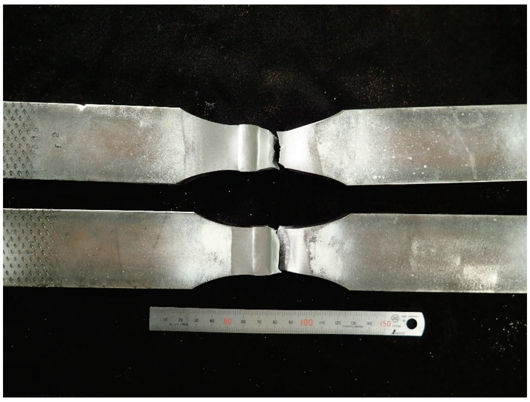

(b) Thickness: 20 mm.

Fig. 21 Tensile test specimens after test.

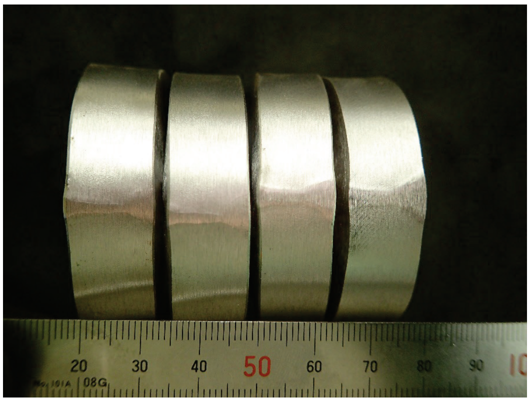

(a) Thickness: 15 mm.

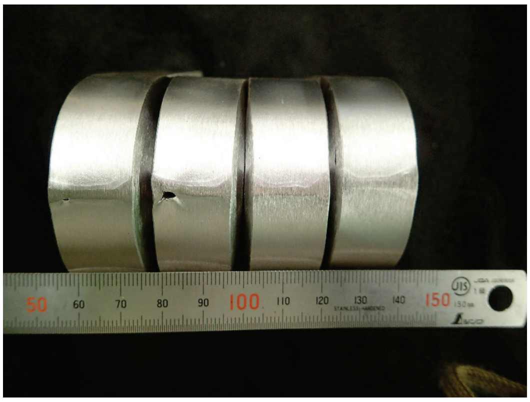

(b) Thickness: 20 mm.

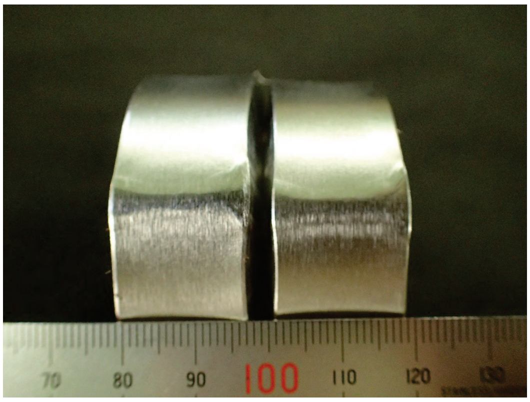

Fig. 23 Retest of bend test for 20 mm-thickness specimens.

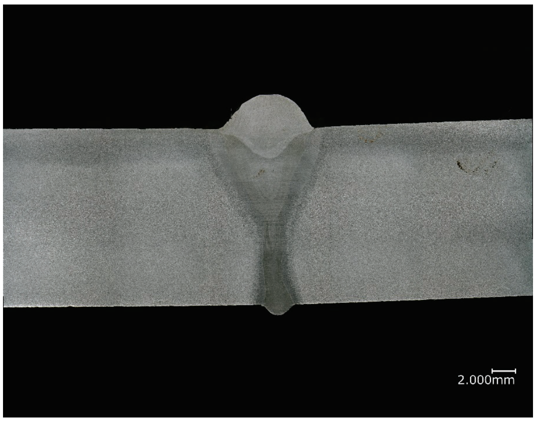

(a) Photograph by macroscopic.

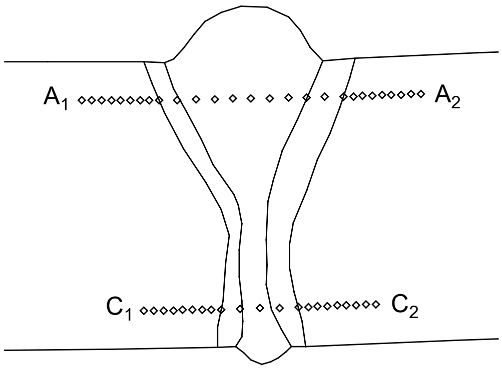

(b) Schematic of measuring points by hardness test.

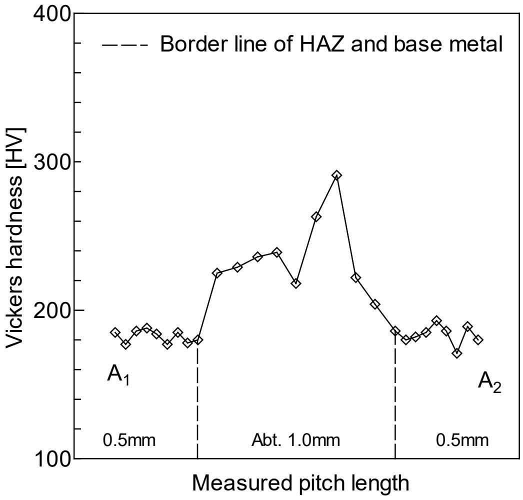

(c) Vickers' hardness test. (A_1A_2 line)

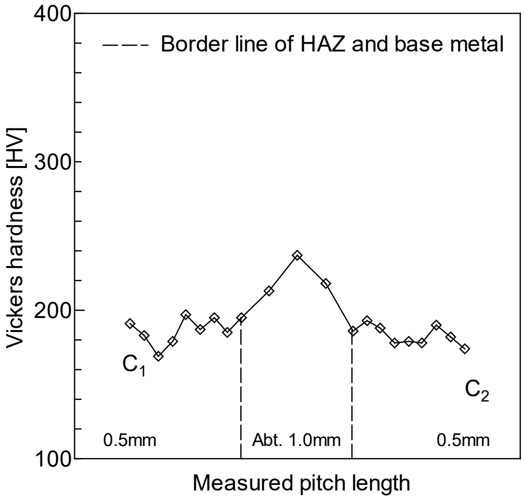

(d) Vickers' hardness test. (C_1C_2 line)

Fig. 24 Macroscopic observation and results of Vickers' hardness test. (Thickness: 15 mm)

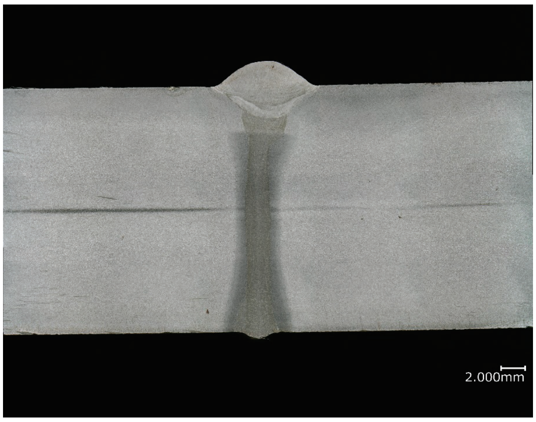

(a) Photograph by macroscopic.

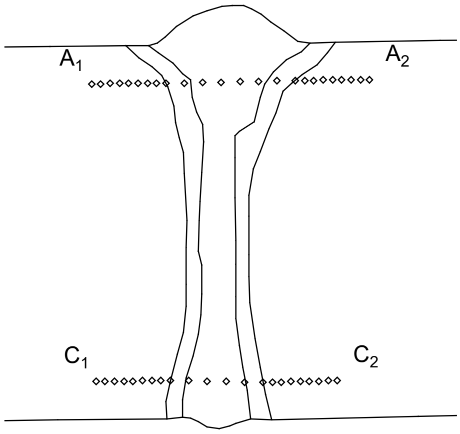

(b) Schematic of measuring points by hardness test.

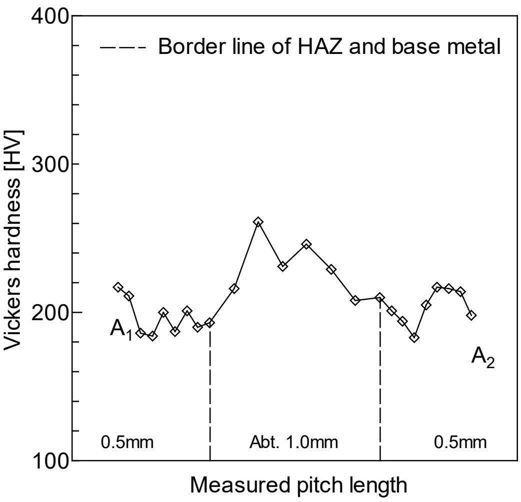

(c) Vickers' hardness test. (A_1A_2 line)

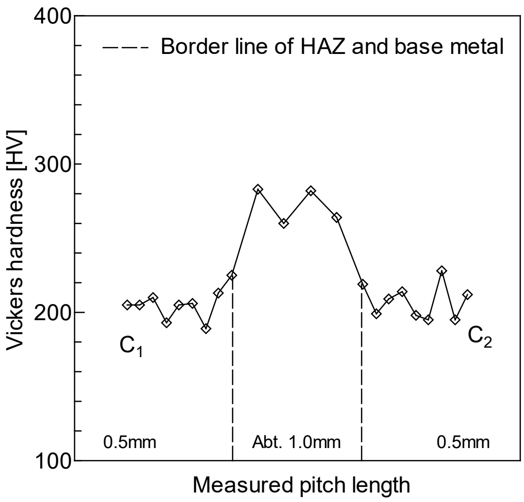

(d) Vickers' hardness test. (C_1C_2 line)

Fig. 25 Macroscopic observation and results of Vickers' hardness test. (Thickness: 20 mm)

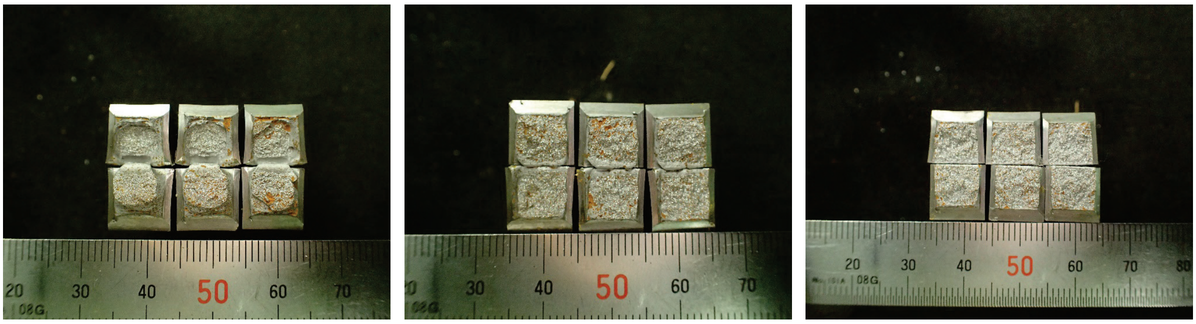

(a) Thickness: 15 mm.

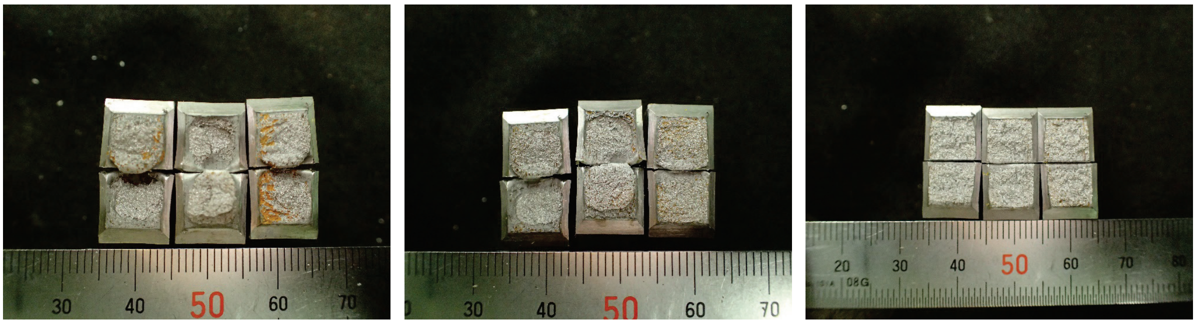

(b) Thickness: 20 mm.

Fig. 26 Impact test specimens.